K-Targeted Metabolomic Analysis Extends Chemical Subtraction to DESIGNER Extracts: Selective Depletion of Extracts of Hops (*Humulus lupulus*)[⊥]

René F. Ramos Alvarenga,† J. Brent Friesen,‡ Dejan Nikolić,† Charlotte Simmler,† José G. Napolitano,† Richard van Breemen,† David C. Lankin,† James B. McAlpine,† Guido F. Pauli†* and Shao-Nong Chen,†*

[†]*UIC/NIH Center for Botanical Dietary Supplements Research, Department of Medicinal Chemistry and Pharmacognosy, College of Pharmacy, University of Illinois at Chicago, Chicago, IL, 60612, United States*

[‡]*Department of Physical Sciences, Rosary College of Art and Sciences, Dominican University, River Forest, IL, 60305, United States*

[⊥]*Residual Complexity and Bioactivity*, Part 24

■ SUPPORTING INFORMATION

TABLE OF CONTENTS *page*

TABLE OF FIGURES *page*

S0. Publication Series *Residual Complexity and Bioactivity*.

The present publication forms *Part 24* in a series of communications on *Residual Complexity and Bioactivity*.

From a **chemical perspective**, residual complexity (RC) refers to the subtle but significant convolution of major and minor chemical species in materials that originate from reaction mixtures, such as natural products. Because natural products are formed biosynthetically, they inherit a certain portion of side products from the metabolomic cocktail. This RC is frequently conserved in highly purified materials, even after an elaborate analytical separation scheme has been applied. The relationship between the biosynthetic cocktail and the products is perpetuated by the RC of the samples. In principle, RC affects all "pure" materials. RCs can be divided into two main groups: static RC describes the thermodynamically stable cases, whereas dynamic RC refers to situations where the impurity patterns change over time due to reactivity or other chemical change that occurs during the timeframe and under the conditions of the observation (e.g., a bioassay).

From a **biological perspective**, RC can have a major impact on bioactivity. Numerous forms of bioassays are widely used for the biological assessment (*in vitro*, *ex vivo*, *in vivo*) of bioactive agents. As many of the bioassays are mechanistically complex by nature, biological evaluation also can be residually complex. This adds a biological layer to the overall RC of bioactive agents and applies to various levels of chemical and biological complexity. Accordingly, both the chemical RC of the agent and the biological RC of the bioassay have to be considered when interpreting information about bioactivity.

As discussed in detail in Part 12 of the publication series (Journal of Natural Products, *75*: 1243-1255 (**2012**); see also below), the recognition and analysis of **RC can help establishing links between the observed biological activity and the underlying chemistry of bioactive agents**. The following table lists the preceding publications since 2008 which establish the publication series *Residual Complexity and Bioactivity*.

Part	**Reference**	**Brief Synopsis Regarding *Residual Complexity and Bioactivity***
Part 1	Jaki BU, Franzblau SG, Chadwick LR, Lankin DC, Zhang F, Wang Y, Pauli GF Purity Bioactivity Relationships – The Case of Anti-TB Active Ursolic Acid Journal of Natural Products **71**: 1742-1748 (**2008**) dx.doi.org/10.1021/np800329j	Demonstrates the relationship between purity, RC and anti-TB activity of different batches of a natural product; uses qHNMR methodology to establish quantitative relationships between purity/RC and activity.
Part 2	Chen S, Turner A, Jaki B, Nikolic D, van Breemen R, Friesen B, Pauli GF An Experimental Implementation of Chemical Subtraction Journal of Pharmaceutical and Biomedical Analysis **46**: 692-698 (**2008**) dx.doi.org/10.1016/j.jpba.2007.12.014	Performs selective removal of a single, interfering phytoconstituent from a bioactive (*E. coli* anti-adherence) fraction and demonstrates the presence of RC in the removed ("subtracted") compound and its assessment by qNMR and MS methods.
Part 3	Schinkovitz A, Pro S, Main M, Chen SN, Jaki BU, Lankin DC, Pauli GF The Dynamic Nature of the Ligustilide Complex Journal of Natural Products **71**: 1606-1611 (**2008**) dx.doi.org/10.1021/np800137n	Shows how RC is generated and varies in purified samples of ligustilide, a designated bioactive marker present in *Angelica* and *Ligusticum* species; compares analytical methods suitable to assess dynamic RC.

Part 4	Gödecke T, Chen SN, Lankin D, Nikolic D, van Breemen R, Pauli GF Phytochemistry of Cimicifugic Acids and Associated Bases in *Cimicifuga racemosa* Root Extracts Phytochemical Analysis **20**: 120-131 (**2009**) dx.doi.org/10.1002/pca.1106	Establishes the new phytochemical methodology that leads to the LC-MS-driven discovery of trace amounts of N-Methyl-serotonin as serotonergic active principle in black cohosh; demonstrates the relevance of low-abundance constituents (RC) as potential bioactive markers for metabolomic mixtures such a botanical extracts.
Part 5	Chen SN, Lankin D, Chadwick L, Jaki B, Pauli GF Dynamic Residual Complexity of Natural Products by qHNMR: Solution Stability of Desmethylxanthohumol Planta Medica *75*: 757-762 (**2009**) dx.doi.org/10.1055/s-0028-1112209	Exemplifies how the dynamic form of RC can lead to the generation of a highly potent phytoestrogen (8-PN) from the inactive precursor (DMX); institutes qHNMR methodology to assess RC in a time-resolved fashion, enabling correlation with bioassay outcome.
Part 6	Pauli GF, Friesen B, Goedecke T, Farnsworth N, Glodny B Occurrence of Progesterone and Related Animal Steroids in Two Higher Plants Journal of Natural Products **73**: 338-345 (**2010**) dx.doi.org/10.1021/np9007415	Unambiguously demonstrates the unexpected occurrence of the mammalian steroid, progesterone, in higher plants and shows that small amounts of this hormone as well as mammalian-like steroid metabolites (e.g., 3-O-sulfates) can form a small but integral part of the RC of plant metabolomes.
Part 7	Molina-Salinas G, Rivas-Galindo V, Said-Fernández S, Lankin D, Muñoz M, Joseph-Nathan P, Pauli GF*, Waksman N* [*corresponding authors] Stereochemical Analysis of Leubethanol, an Anti-TB Active Serrulatane, from *Leucophyllum frutescens* Journal of Natural Products **74**: 1842-1850 (**2011**) dx.doi.org/10.1021/np2000667	Establishes the subtle but significant diastereomeric difference between elisabethanol, which had been isolated from a gorgonian organism, and leubethanol, the anti-TB active lead compound from a plant; utilizes VCD for the determination of absolute stereochemistry and emphasizes ^{1}H iterative full spin analysis (HiFSA) as a dereplication tool and for the analysis of RC of natural products.
Part 8	Gödecke T, Napolitano J, Yao P, Nikolic D, Dietz B, Bolton J, van Breemen R, Chen SN, Lankin D, Farnsworth N, Pauli GF Integrated Standardization Concept for *Angelica* Botanicals using Quantitative NMR Fitoterapia *83*: 18-32 (**2012**) dx.doi.org/10.1016/j.fitote.2011.08.017	Establishes a qHNMR-based protocol for the simultaneous quantitation of multiple marker compounds in the bioactive fraction ([anti-]estrogenicity, cytotoxicity) of *Angelica sinensis* botanicals; demonstrates the advanced role qHNMR can have in botanical standardization and evaluation of RC of the plant extracts.
Part 9	Qiu F, Imai A, McAlpine J, Lankin D, Burton I, Karakach T, Farnsworth N, Chen SN, Pauli GF	Determines the RC of purified botanical reference materials of triterpenes from black cohosh; demonstrates the assessment

	Dereplication, Residual Complexity and Rational Naming - the Case of the *Actaea* Triterpenes Journal of Natural Products **75**: 432-443 (**2012**) dx.doi.org/10.1021/np200878s	of RC by computer-aided dereplication using classification binary trees (CBTs) to derive both structural information and quantitative measures for minor components contained in residually complex samples.
Part 10	Napolitano J, Gödecke T, Rodriguez Brasco MF, Jaki BU, Chen SN, Lankin DC, Pauli GF The Tandem of Full Spin Analysis and qHNMR for the Quality Control of Botanicals Exemplified with **Ginkgo biloba** Journal of Natural Products **75**: 238-248 (**2012**) dx.doi.org/10.1021/np200949v	Establishes ^{1}H iterative full spin analysis (HiFSA) as the basis of a qHNMR approach for the parallel quantitation of eight bioactive markers in *Ginkgo biloba*; exemplifies how multi-target standardization can be achieved without the need for identical calibrants in (residually) complex samples including reference materials, fractions, and extracts; addresses the role of RC in reference materials of calibrants.
Part 11	Qiu F, Friesen JB, McAlpine JB, Pauli GF NMR-based Design of Countercurrent Separation of *Ginkgo biloba* Terpene Lactones Journal of Chromatography A **1242**: 26-34 (**2012**) dx.doi.org/10.1016/j.chroma.2012.03.081	Introduces qHNMR in both the design and the analysis of countercurrent separation (CS) of bioactive botanical markers; demonstrates the measurement of partition coefficients of target markers in mixtures; evaluates chromatographic orthogonality in CS; establishes quantitative links between predicted and experimental CS performance and the RC of the purified markers.
Part 12	Pauli GF**,** Chen SN, Friesen JB, McAlpine J, Jaki BU Analysis and Purification of Bioactive Natural Products - The AnaPurNa Study Journal of Natural Products **75**: 1243-1255 (**2012**) dx.doi.org/10.1021/np300066q	Comprehensive meta-analysis of the literature (1999-2010) focusing on the role of analytical methodology in the purification and characterization of bioactive compounds from natural sources; addresses the role of RC in their purification and characterization and discusses the impact of RC on the biological evaluation and validation of lead compounds.

Part 13	Napolitano J, Lankin D, Chen SN, Pauli GF Complete ^{1}H NMR Spectral Analysis of Ten Chemical Markers of *Ginkgo biloba* Magnetic Resonances in Chemistry **50**: 569-575 (**2012**) dx.doi.org/10.1002/mrc.3829	Establishes the methodology for the generation of unambiguous ^{1}H NMR fingerprints of bioactive markers, exemplified for terpene lactones and flavonoids from *Ginkgo biloba*; the fingerprints are suitable for both structural dereplication and qHNMR quantitation at various levels of RC, can be scaled to all existing NMR field strength, and are independent of instrumentation.
Part 14	Riihinen K, Gödecke T, Pauli GF Purification of Berry Flavonoids by Long-bed Gel Permeation Chromatography Journal of Chromatography A, *1244*: 20-27 (**2012**) dx.doi.org/10.1016/j.chroma.2012.04.060	Establishes long-bed gel permeation chromatography (GPC) on Sephadex LH-20 as an efficient method for the purification of bioactive berry polyphenols; despite its capability to resolve closely related compounds, qHNMR analysis reveals an un expected degree of RC in the GPC fractions.
Part 15	Inui T, Wang Y, Pro S, Franzblau SG, Pauli GF Unbiased Evaluation of Bioactive Secondary Metabolites in Complex Matrices Fitoterapia **83**: 1218-1225 (**2012**) dx.doi.org/10.1016/j.fitote.2012.06.012	Establishes biochemometric methodology capable of identifying bioactive principles in crude metabolomic mixtures, as an alternative to bioassay-guided fractionation; establishes chemometric links between the bioassay and the preparative and analytical chemistry of (residually) complex natural products; exemplifies the concept for the anti-TB active principles of the ethnobotanical, *Oplopanax horridus*.
Part 16	Dong SH, Nikolic D, Simmler C, Qiu F, van Breemen RB, Soejarto DD, Pauli GF, Chen SN Diarylheptanoids from *Dioscorea villosa* (Wild Yam) Journal of Natural Products *75*: 2168-2177 (**2012**) dx.doi.org/10.1021/np300603z	Establishes a link between the ubiquitous RC of crude metabolomes of *Dioscorea villosa* and the approach of qHNMR-guided metabolomic mining of the minor diarylheptanoid constituents; extends the utility of qHNMR applications and complements previous conclusions about the broader relevance of RC; HiFSA profiles of the isolates lay the groundwork for the quantifiable assessment of the RC of *Dioscorea* botanical preparations.

Part 17	Qiu F, Cai G, Jaki BU, Lankin DC, Franzblau SG, Pauli GF Quantitative Purity-Activity Relationships of Natural Products: The Case of Anti-Tuberculosis Active Triterpenes from *Oplopanax horridus* Journal of Natural Products *76*: 413-419 (**2013**) http://dx.doi.org/10.1021/np3007809	Extends the previously developed concept of purity–activity relationships (PARs) for the *quantitative* evaluation of the effects of multiple minor components on the bioactivity of residually complex natural products; presents the anti-tuberculosis triterpenes of *Oplopanax horridus* as a case for the development of the quantitative PAR (QPAR) concept; characterizes the RC of the purified triterpenes combined w/structurally related and unrelated impurities by 1D/2D-NMR; uses biochemometric methodology to study the qHNMR purity and anti-TB activity of successive chromatographic fractions of *O. horridu*s triterpenes and generate a mathematical QPAR model by linear regression analysis. QPAR enables a *quantitative* assessment when RC affects the biological activity of natural products.
Part 18	Simmler C, Hajirahimkhan A, Lankin DC, Bolton J, Jones T, Soejarto D, Chen SN, Pauli GF Dynamic Residual Complexity of the Isoliquiritigenin-Liquiritigenin Interconversion During Bioassay Journal of Agricultural and Food Chemistry *61*: 2146-2157 (**2013**) http://dx.doi.org/10.1021/jf304445p	Demonstrates the relevance of the dynamic residual complexity of chalcones and flavanones under in vitro bioassay conditions by time-resolved investigation of the isomerization of isoliquiritigenin and liquiritigenin in cell culture media, with and without cells; shows that isomerization leads to equilibrium mixtures with enantiomeric excess of the R-flavanone. The findings underscore the importance of choice and definition of in situ conditions in biological test systems as they affect chemical reactivity and, thus, the RC of test agents.

Part 19	Gödecke T, Napolitano JG, Rodriguez Brasco MF, Chen SN, Jaki BU, Lankin DC, Pauli GF Validation of a Generic qHNMR Method for Natural Products Analysis Phytochemical Analysis *24*: in press (**2013**) http://dx.doi.org/10.1002/pca.2436	Introduces a validated protocol for quantitative ^{1}H NMR (qHNMR) analysis of complex samples with relatively high dynamic range. Comprehensive coverage of acquisition and processing parameters as well as software, and specific attention to the requirements of natural products makes the protocol suitable for a wide range of analytes and applications, from the quality control of highly complex crude botanical extracts to the assessment of the purity and residual complexity of reference compounds.
Part 20	Napolitano JG, Lankin D, Graf T, Friesen JB, Chen SN, McAlpine JB, Oberlies, NH, Pauli GF HiFSA Fingerprinting of Isomers with Near Identical NMR Spectra: The Silybin/Isosilybin Case The Journal of Organic Chemistry *78*: 2827-2839 (**2013**) http://dx.doi.org/10.1021/jo302720h	Demonstrates how the "hidden" complexity of regio- and diastereoisomers with near-identical NMR spectra can be distinguished and unambiguously assigned by quantum mechanical driven, ^{1}H iterative Full Spin Analysis (HiFSA); illustrates the method with the four main flavonolignans of *Silybum marianum* ([iso]silybins A/B) which have posed an analytical challenge for nearly six decades. The highly reproducible HiFSA ^{1}H NMR fingerprints allow distinction of the near-identical our isomers at ^{1}H frequencies from 300 to 900 MHz and parallel quantification, even in difficult to characterize mixtures. HiFSA methodology opens new opportunities to explore "hidden" RC and diversity in the chemical space of organic molecules.
Part 21	Dong SH, Cai G, Napolitano JG, Nikolic N, Lankin DC, McAlpine JB, van Breemen R, Soejarto DD, Pauli GF, Chen SN Lipidated Steroid Saponins from *Dioscorea villosa* Fitoterapia *91*: 113-124 (2013) dx.doi.org/10.1016/j.fitote.2013.07.018	Continues the use of metabolomic mining and establishes a series of difficult to purify and analyze lipidated steroid saponins; the discovery of highly lipophilic, aliphatic esters as new markers of the widely used botanical, *D. villosa*; provides new perspectives for the potential biological roles of the otherwise relatively polar steroid glycosides and related phytoconstituents.

Part 22	Qiu F, McAlpine J, Lankin D, Burton I, Karakach T, Chen SN, Pauli GF 2D NMR Barcoding and Differential Analysis of Complex Mixtures for Chemical Identification: the Actaea Triterpenes Analytical Chemistry 86: 3964-3972 (2014) dx.doi.org/10.1021/ac500188j	Similar to general barcoding technology, 2D-NMR barcoding utilizes clusters of fingerprint signals for the direct analysis of complex mixtures. It enables the identification of both known and new structures according to their structural subtypes. Demonstrated for HMBC data, 2D-NMR barcoding uses the structural information encoded in the 2-D chemical shift space in the form of relative cross peak patterns. The specificity of the patterns enables the distinction between congeneric metabolites in (residually) complex mixtures from extracts to purified compounds.
Part 23	Riihinen K, Ou Z, Goedecke T, Lankin D, Pauli GF, Wu C The Antibiofilm Activity of Lingonberry Flavonoids against Oral Pathogens is a Case Connected to Residual Complexity Fitoterapia *97,* 78-86 (2014) dx.doi.org/10.1016/j.fitote.2014.05.012	The antimicrobial activity of isolated lingonberry flavonoid glycosides could not be confirmed with identical reference materials from other source. Representing a case of both static and dynamic residual complexity, even after HPLC-PDA, NMR, and MALDI-TOF analyses, the structural identity of the bioactive minor constituents in the cranberry-derived bioactive markers remained unknown, while color and analytical characteristics point to flavonoid oxidation products as underlying active principles.

S1. Overview of the Biological Activities of the Target Metabolites 1-4 from Hops

Preparations of isoxanthohumol (**1**), a prenylated flavanone found as the isomerization product of **4**, were shown to exhibit the following activities: weak estrogenic,[1] antiproliferative in breast and ovarian cancer cell lines,[2] antitumor,[3] and suppression of the synthesis and release of pro-inflammatory cytokines.[10] Whereas, preparations of its demethylated derivative, 8-prenylnaringenin (**2**), found only in traces amounts, has been characterized as being the most potent phytoestrogen in hops,[4,5] binding both α- and β- estrogen receptors,[6] as a result of being an apoptosis inducer and an inhibitor of cell cycle progression in human breast cancer cells MCF-7.[7,8] Although closely structurally related to **2**, 6-prenylnaringenin (**3**) shows a lower potency in binding to estrogen receptors,[5,9] but has inhibitory effects against skin-tumor promotion in a mouse skin carcinogenesis model.[10] This compound also has exhibited induction of a caspase-independent cell death in the PC-3 and DU145 prostate cancer cell lines,[11] and has potential as an inhibitor of human 20S proteasome.[12]

Preparations containing xanthohumol (**4**), a major hops resin constituent, have shown pleiotropic chemopreventive activity.[13] Multiple biological activities have been attributed to **4**: antiproliferative activity in breast,[2] ovarian[2,14] and colon cell lines,[15] apoptosis induction in malignant glioblastoma cells,[16] BPH-1 prostate cells,[17] breast cancer cell lines,[18]and antiproliferative activity in PC-3 and DU145 prostate cancer cell lines.[19] Furthermore, **4** has been reported as an aromatase inhibitor, a quinone reductase 1 (NQO1) inducer,[20] an inhibitor of cholesteryl ester transfer protein,[21] and a potential anti-inflammatory agent through inhibition of NF-κβ transactivation and inhibition of STAT-1α and IRF-1.[22]

References

(1) Overk, C. R.; Yao, P.; Chadwick, L. R.; Nikolic, D.; Sun, Y.; Cuendet, M. A; Deng, Y.; Hedayat, A.S.; Pauli, G. F.; Farnsworth, N. R.; van Breemen, R.B.; Bolton, J.L. *J. Agric. Food Chem.* **2005**, *53*, 6246–6253.

(2) Miranda, C. L.; Stevens, J. F.; Helmrich, A.; Henderson, M. C.; Rodriguez, R. J.; Yang, Y.; Deinzer, M.; Barnes, D.; DR, B. *Food Chem. Toxicol.* **1999**, *37*, 271–285.

(3) Serwe, A.; Rudolph, K.; Anke, T.; Erkel, G. *Invest. New Drugs* **2012**, *30*, 898–915.

(4) Milligan, S. R.; Kalita, J. C.; Heyerick, A.; Rong, H.; De Cooman, L.; De Keukeleire, D. *J. Clin. Endocrinol. Metab.* **1999**, *83*, 2249–2252.

(5) Milligan, S. R.; Kalita, J. C.; Pocock, V.; Van de Kauter, V.; Stevens, J. F.; Deinzer, M. . L.; Rong, H.; De Keukeleire, D. *J. Clin. Endocrinol. Metab.* **2000**, *85*, 4912–4915.

(6) Milligan, S.; Kalita, J.; Pocock, V.; Heyerick, a; De Cooman, L.; Rong, H.; De Keukeleire, D. *Reproduction* **2002**, *123*, 235–242.

(7) Brunelli, E.; Minassi, A.; Appendino, G.; Moro, L. *J. Steroid Biochem. Mol. Biol.* **2007**, *107*, 140–148.

(8) Brunelli, E.; Pinton, G.; Chianale, F.; Graziani, A.; Appendino, G.; Moro, L. *J. Steroid Biochem. Mol. Biol.* **2009**, *113*, 163–170.

(9) Effenberger, K. E.; Johnsen, S. a; Monroe, D. G.; Spelsberg, T. C.; Westendorf, J. J. *J. Steroid Biochem. Mol. Biol.* **2005**, *96*, 387–399.

(10) Akazawa, H.; Kohno, H.; Tokuda, H.; Suzuki, N.; Yasukawa, K.; Kimura, Y.; Manosroi, A.; Manosroi, J.; Akihisa, T. *Chem. Biodivers.* **2012**, *9*, 1045–1054.

(11) Delmulle, L.; Berghe, T. Vanden; Keukeleire, D. De; Vandenabeele, P. *Phyther. Res.* **2008**, *203*, 197–203.

(12) Kim, Y.; Lee, H.; Park, E.; Shim, S. H. *Bull.Korean Chem. SOc.* **2009**, *30*, 1867–1869.

(13) Gerhauser, C.; Alt, A.; Heiss, E.; Gamal-eldeen, A.; Klimo, K.; Knauft, J.; Neumann, I.; Scherf, H.; Frank, N.; Bartsch, H.; Becker, H. *Mol. Cancer Ther.* **2002**, *1*, 959–969.

(14) Drenzek, J. G.; Seiler, N. L.; Jaskula-Sztul, R.; Rausch, M. M.; Rose, S. L. *Gynecol. Oncol.* **2011**, *122*, 396–401.

(15) Pan, L.; Becker, H.; Gerhäuser, C. *Mol. Nutr. Food Res.* **2005**, *49*, 837–843.

(16) Festa, M.; Capasso, A.; Acunto, C. W. D.; Masullo, M.; Rossi, A. G.; Pizza, C.; Piacente, S. *J. Nat. Prod.* **2011**, *11*, 2505–2513.

(17) Colgate, E. C.; Miranda, C. L.; Stevens, J. F.; Bray, T. M.; Ho, E. *Cancer Lett.* **2007**, *246*, 201–209.

(18) Monteiro, R.; Faria, A.; Azevedo, I.; Calhau, C. *J. Steroid Biochem. Mol. Biol.* **2007**, *105*, 124–130.

(19) Delmulle, L.; Bellahcène, A.; Dhooge, W.; Comhaire, F.; Roelens, F.; Huvaere, K.; Heyerick, A.; Castronovo, V.; De Keukeleire, D. *Phytomedicine* **2006**, *13*, 732–734.

(20) Dietz, B. M.; Kang, Y.-H.; Liu, G.; Eggler, A. L.; Yao, P.; Chadwick, L. R.; Pauli, G. F.; Farnsworth, N. R.; Mesecar, A. D.; van Breemen, R. B.; Bolton, J. *Chem. Res. Toxicol.* **2005**, *18*, 1296–1305.

(21) Hirata, H.; Takazumi, K.; Segawa, S.; Okada, Y.; Kobayashi, N.; Shigyo, T.; Chiba, H. *Food Chem.* **2012**, *134*, 1432–1437.

(22) Cho, Y.-C.; Kim, H. J.; Kim, Y.-J.; Lee, K. Y.; Choi, H. J.; Lee, I.-S.; Kang, B. Y. *Int. Immunopharmacol.* **2008**, *8*, 567–573.

S2. NMR Profiles of Subtracted Compounds 1, 2/3, and 4 – First CS Subtraction Step

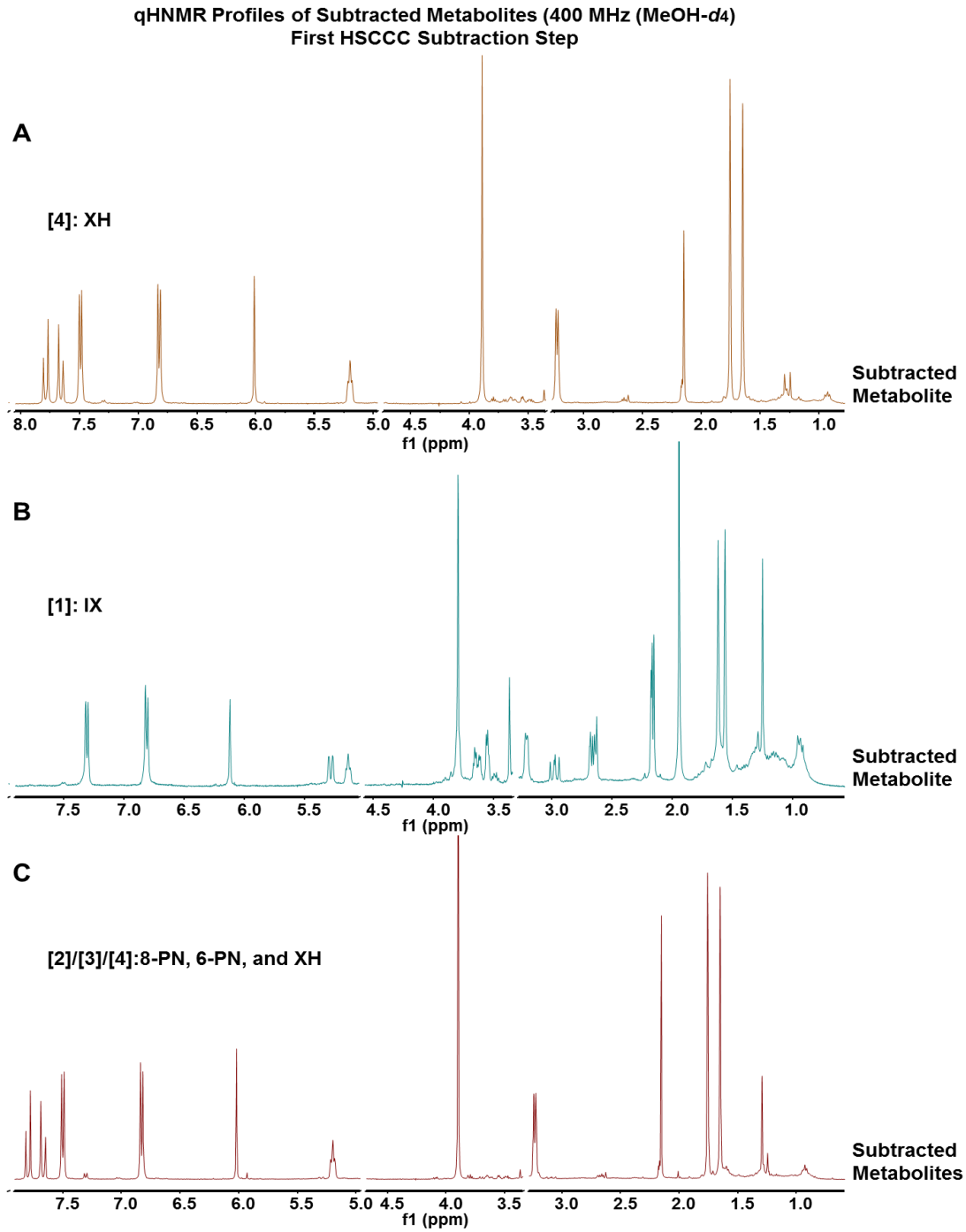

Figure S2. NMR profiles of subtracted compounds – First CS subtraction step. The NMR measurements were done in MeOH-d_4 in a Bruker NMR AVANCE-400 MHz under quantitative conditions (qHNMR). Panel A: qHNMR profile of subtracted metabolite **4** (XH) with a purity of 90.08% w/w after first CS subtraction step. Panel B: qHNMR profile of subtracted metabolite **1** (IX) with a purity of 54.55% w/w after first CS step. Panel C: qHNMR profile of subtracted fraction containing the coeluting metabolites 2-4, where compound **2** was 3.45% w/w, compound 3 was 4.25% w/w, and compound **4** account for 91.14 % w/w, after first CS step. The CS solvent system applied was HEMWat 0. Water and solvent peaks were removed.

S3. NMR Profiles of Total Extract, DESIGNER Extracts, and Subtracted Compounds 1 and 2/3

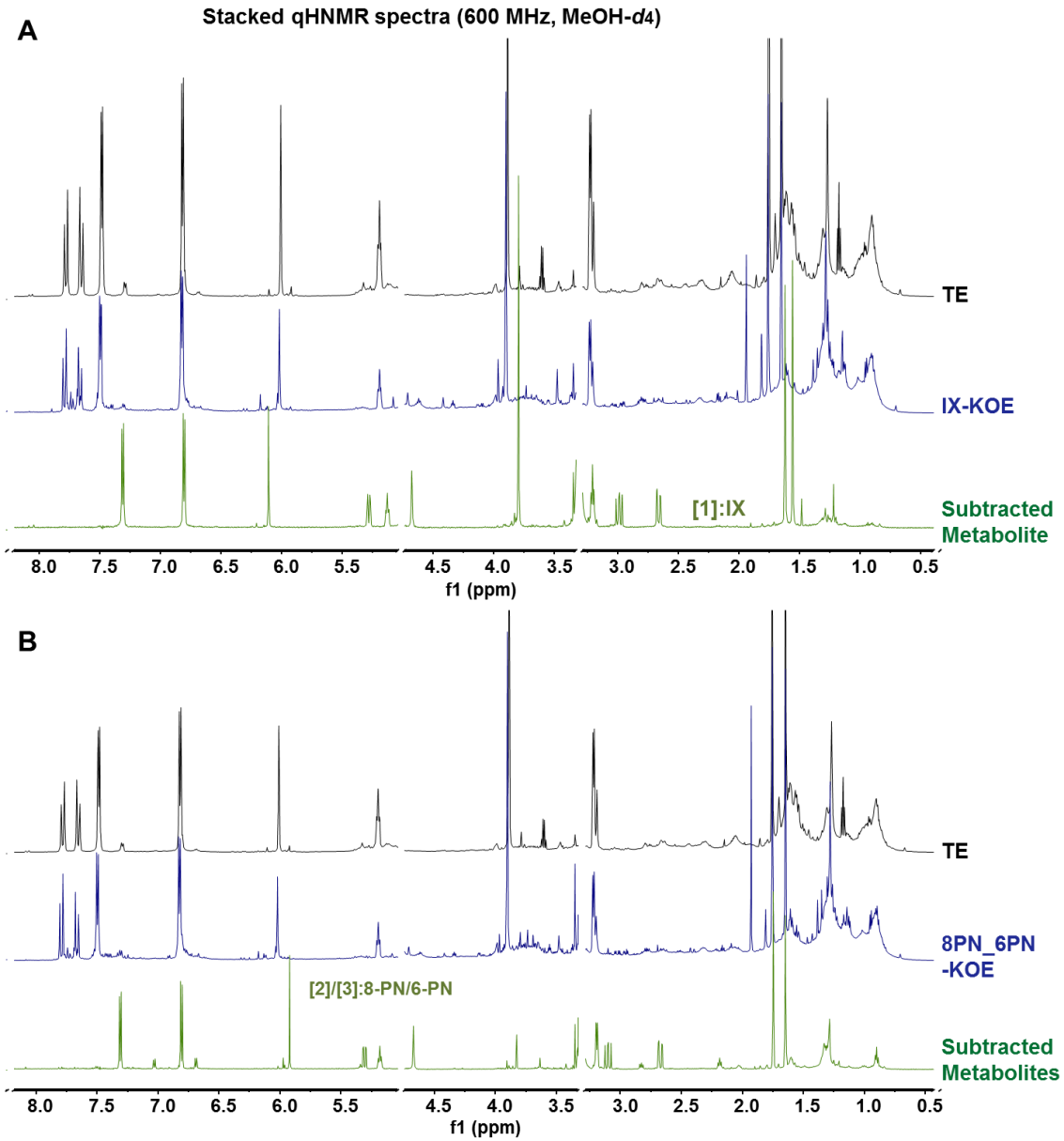

Figure S3. qHNMR profiles of total extract (TE), DESIGNER extracts (Ts-DE), and subtracted metabolites. The NMR measurements were done in MeOH-d_4 in a Bruker NMR AVANCE-600 MHz under quantitative conditions (qHNMR). Panel **A**: Comparison of NMR profiles of total extract (in black) vs. isoxanthohumol (**1**) DESIGNER extract or IX-DE (in blue), and subtracted metabolite **1** (in green) after second CS step. Subtracted metabolite 4 is shown to have been depleted from the total extract (TE) when compared to its respective DESIGNER extract (XH-DE). The qHNMR final purity of subtracted metabolite **1** corresponds to 94.67% w/w, calculated by applying the 100% method. **Panel B**: Comparison of NMR profiles of total extract (in black) vs. 8-PN/6-PN-DE (in blue), and subtracted metabolites **2-3** (in green) after second CS step. Based on the 100% method, the subtracted fraction contains 1.28% w/w of metabolite 2, and 66.04% w/w of metabolite **3**. Water and solvent peaks were removed.

S4. NMR Profile of Subtracted Metabolites (Ts) – MultiT - First CS Subtraction Sstep

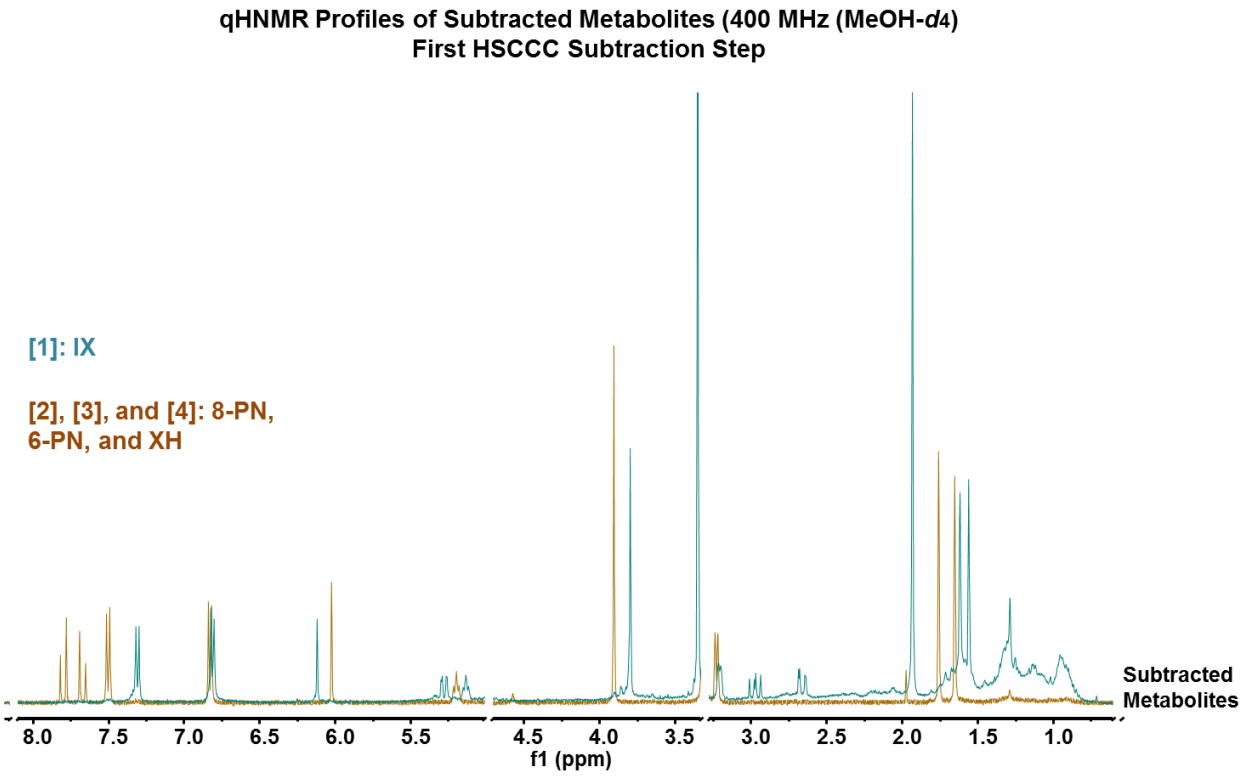

Figure S4. The NMR measurements were done in MeOH-d_4 in a Bruker NMR AVANCE-400 MHz under 1quantitative conditions (qHNMR). qHNMR profiles of subtracted metabolite **1** (IX: in cyan blue) with a purity of 58.82% w/w, and the qHNMR profile of subtracted fraction containing the coeluting metabolites **2**-**4** (8-PN, 6-PN, and XH; in dark orange), where compound **2** was 1.97% w/w, compound **3** was 4.11% w/w, and compound **4** account for 93.00% w/w, after first CS step. The CS solvent system applied was HEMWat 0. Water and solvent peaks were removed.

S5. LC-MS Profiles of Subtracted Metabolites: Xanthohumol (4, XH) and Isoxanthohumol (1, IX)

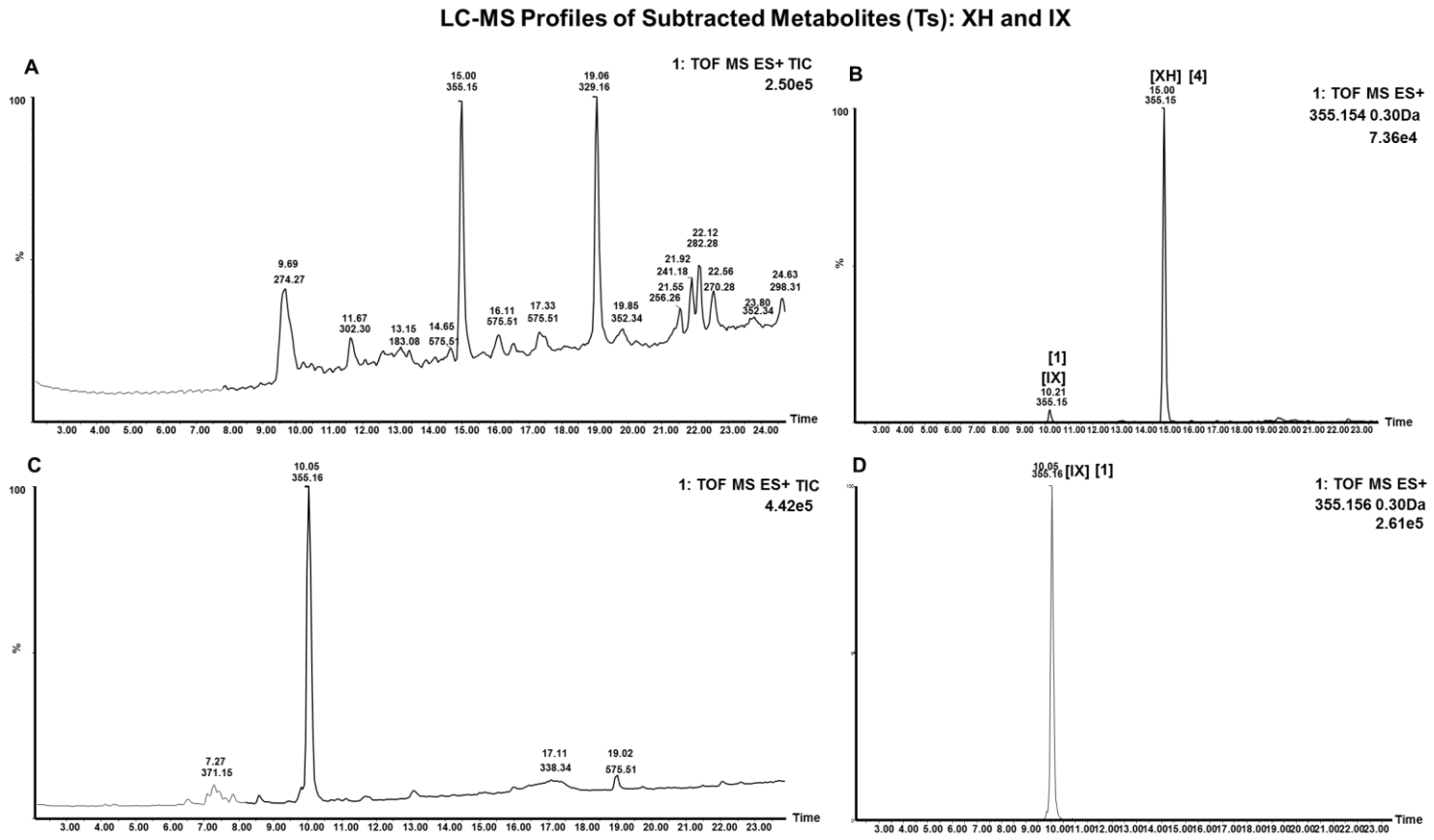

Figure S5. LC-MS Profiles of subtracted metabolites . **Panel A**: Total ion chromatogram (TIC) of subtracted metabolite **4**. The baseline noise is a result of carryover from previous eluents on the column. **Panel B**: Extracted ion chromatogram in positive mode (ES+) from subtracted fraction containing metabolite **4,** at *m/z* = 355.15. The presence of the isomerization product of **4**, compound **1**, can be seen. **Panel C**: TIC of subtracted metabolite **1**. **Panel D**: ES+ at *m/z* = 355.15 from subtracted fraction containing metabolite **1**. Qualitative LC-MS-MS analyses were carried out using Waters (Milford, MA) 2695 solvent delivery system connected to a Waters SYNAPT quadrupole/time-of-flight mass spectrometer operated in positive ion electrospray mode. HPLC separations were carried out using a Waters XBridge C_{18} reversed phase column (2.0 x 50 mm, 2.5 µm) and a mobile phase consisting of 0.1% aqueous formic acid (solvent A) and MeCN (solvent B). Compounds were separated using a linear gradient from 20-80%B over 15 min at a flow rate of 0.22 mL/min. Mass spectrometric data were acquired from *m/z* 150-800 at 10,000 FWHM resolution using Leu-enkephalin as the lock mass. Tandem mass spectra were taken at 15eV or 25 eV using argon as collision gas.

S6. LC-MS Profiles of Subtracted Metabolites: Xanthohumol (4, XH) and Isoxanthohumol (1, IX) - MultiT-DE

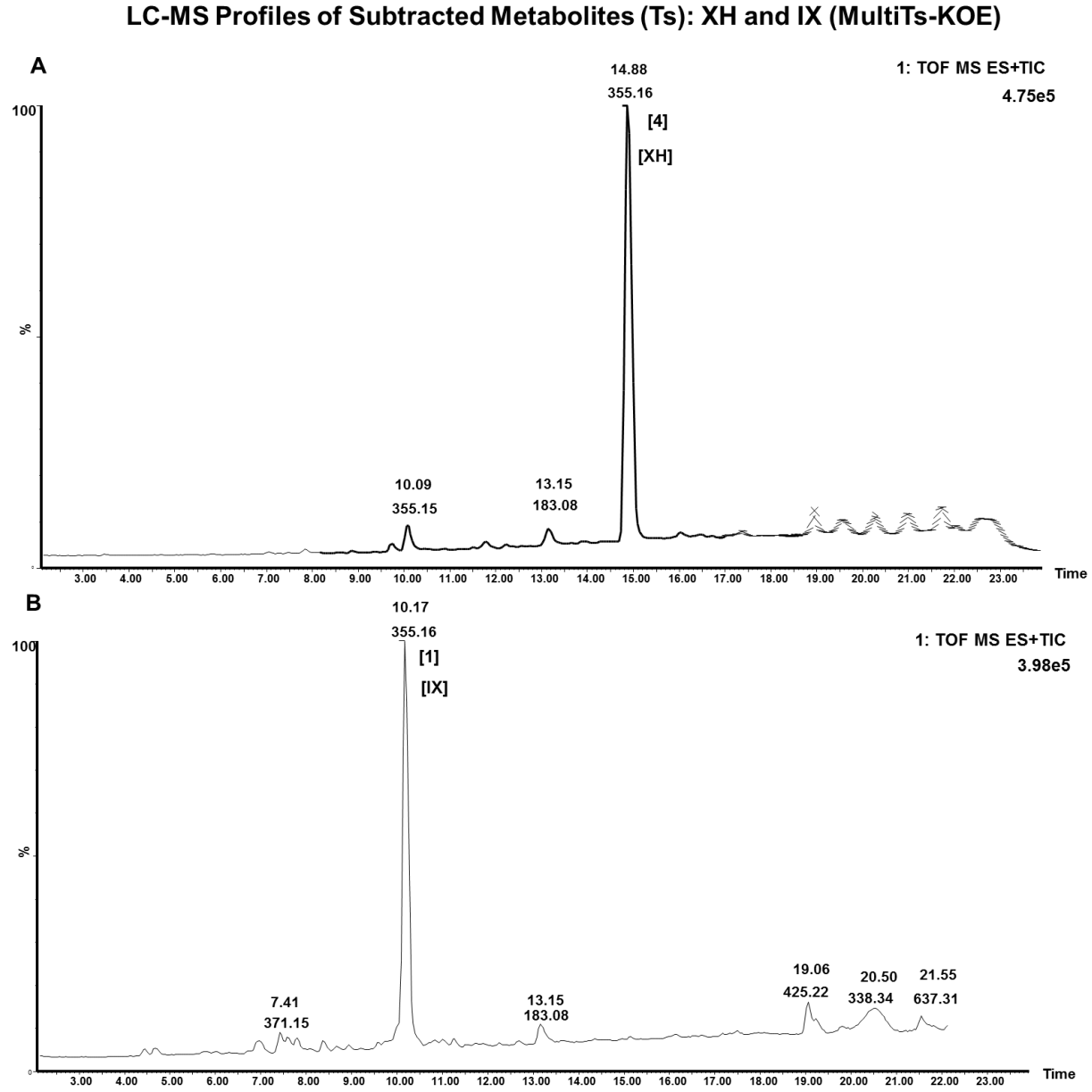

Figure S6. LC-MS Profiles of subtracted metabolites: xanthohumol XH (**4**) and isoxanthohumol IX (**1**) - MultiT-DE. **Panel A**: Total ion chromatogram (TIC) of subtracted metabolite **4**. **Panel B**: Total ion chromatogram (TIC) of subtracted metabolite **1**. Qualitative LC-MS-MS analyses were carried out using Waters (Milford, MA) 2695 solvent delivery system connected to a Waters SYNAPT quadrupole/time-of-flight mass spectrometer operated in positive ion electrospray mode. HPLC separations were carried out using a Waters XBridge C18 reversed phase column (2.0 x 50 mm, 2.5 µm) and a mobile phase consisting of 0.1% aqueous formic acid (solvent A) and MeCN (solvent B). Compounds were separated using a linear gradient from 20-80% B over 15 min at a flow rate of 0.22 mL/min. Mass spectrometric data were acquired from m/z 150-800 at 10,000 FWHM resolution using Leu-enkephalin as the lock mass. Tandem mass spectra were taken at 15 eV or 25 eV using argon as collision gas.

S7. LC-MS Profiles of Subtracted Metabolites: 8-Prenylnaringenin (2, 8-PN) and 6-Prenylnaringenin (3, 6-PN) – 8-PN/6-PN-DE and MultiT-DE

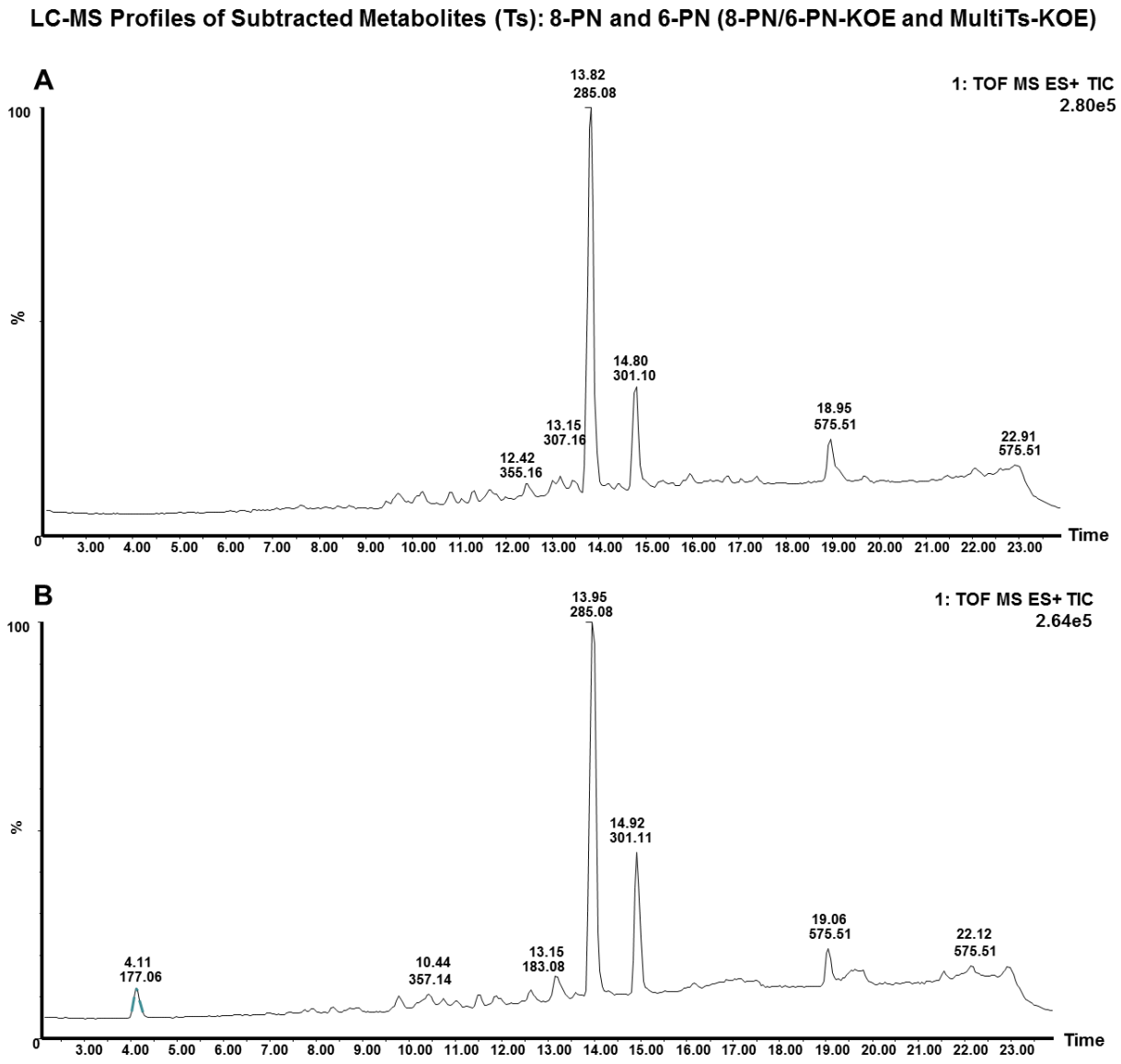

Figure S7. LC-MS profiles of subtracted metabolites: 8-prenylnaringenin 8-PN (**2**) and 6-prenylnaringenin 6-PN (**3**) – 8-PN/6-PN-DE and MultiT-DE. Qualitative LC-MS-MS analyses were carried out using Waters (Milford, MA) 2695 solvent delivery system connected to a Waters SYNAPT quadrupole/time-of-flight mass spectrometer operated in positive ion electrospray mode. HPLC separations were carried out using a Waters XBridge C18 reversed phase column (2.0 x 50 mm, 2.5 µm) and a mobile phase consisting of 0.1% aqueous formic acid (solvent A) and MeCN (solvent B). Compounds were separated using a linear gradient from 20-80%B over 15 min at a flow rate of 0.22 mL/min. Mass spectrometric data were acquired from m/z 150-800 at 10,000 FWHM resolution using Leu-enkephalin as the lock mass. Tandem mass spectra were taken at 15eV or 25 eV using argon as collision gas.

S8. UHPLC-UV Profiles of Total Extract (TE) vs. Xanthohumol (4, XH)-knock out Extract (XH-DE).

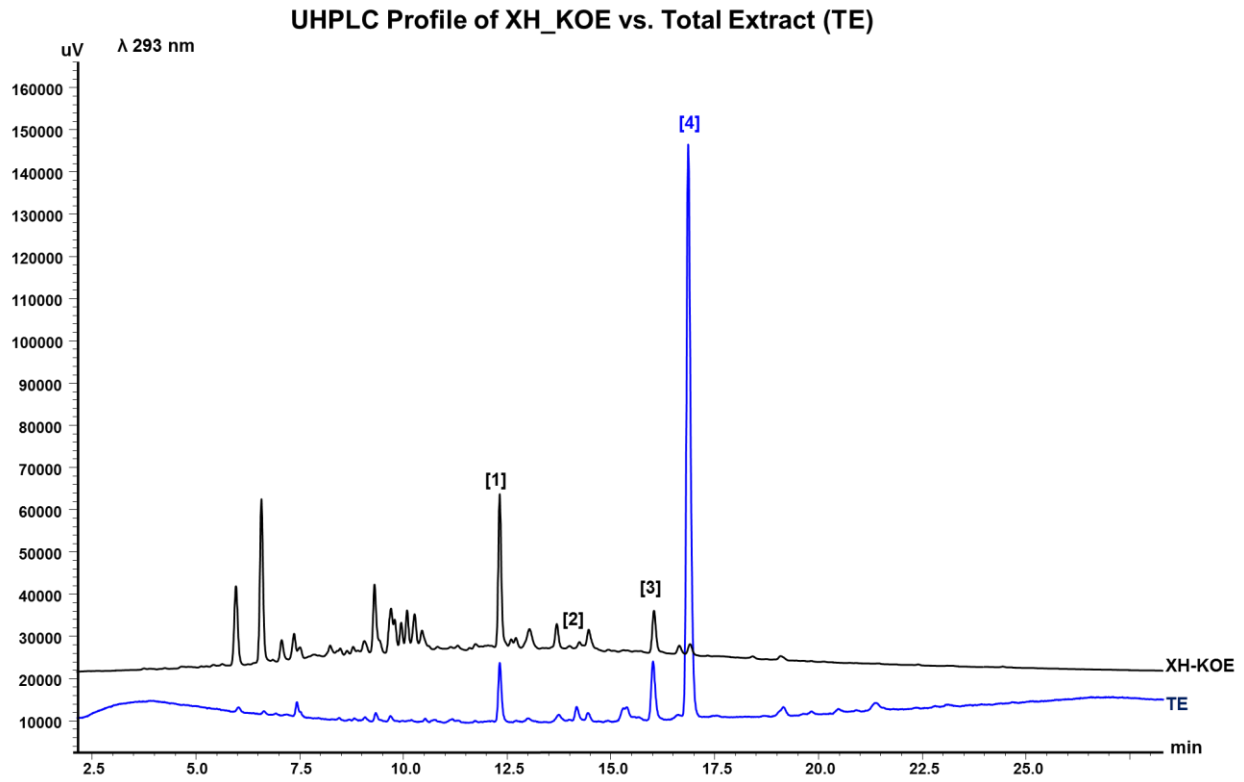

Figure S8. UHPLC-UV profile of total extract (TE) vs. XH-DE. Compounds were eluted on a Waters Acquity UPLC® BEH C18 (2.1 x 5.0 mm, 1.7µm) column using the following gradient A: H_2O, B: MeCN + 0.1% HCO_2H (Formic acid) from 5% to 57% B in 18 min, from 57% to 98 % B in 7 min, isocratic mode at 98 % B and during 3 min at a flow rate of 0.6 mL/ min. Under those conditions, the retention times of (**1**) to (**4**) were 12.2 min, 14.2 min, 16.0 min, and 16.9 min, respectively. In blue, the total extract is shown. In black, the respective DE (XH-DE) is shown. Target metabolite **4** shows to be highly removed from the total extract to produce the DE.

S9. UHPLC-UV Profiles of Total Extract (TE) vs. Isoxanthohumol (1, IX)-Knock out extract (IX-DE).

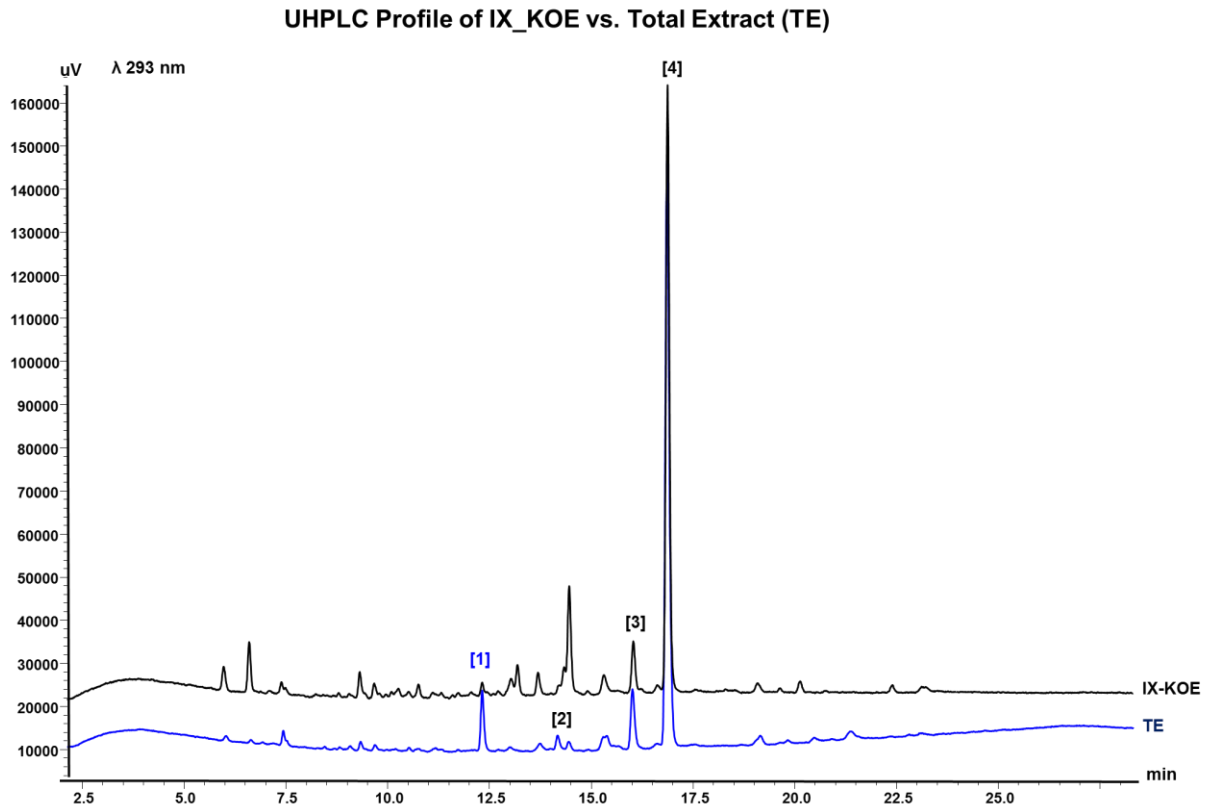

Figure S9. UHPLC-UV profile of total extract (TE) vs. IX-DE. Compounds were eluted on a Waters Acquity UPLC® BEH C18 (2.1 x 5.0 mm, 1.7µm) column using the following gradient A: H_2O, B: MeCN + 0.1% HCO_2H (Formic acid) from 5% to 57% B in 18 min, from 57% to 98 % B in 7 min, isocratic mode at 98 % B and during 3 min at a flow rate of 0.6 mL/ min. Under those conditions, the retention times of (**1**) to (**4**) were 12.2 min, 14.2 min, 16.0 min, and 16.9 min, respectively. In blue, the total extract is shown. In black, the respective DE (IX-DE) is shown. Target metabolite **1** shows to be highly removed from the total extract to produce the DE.

S10. UHPLC-UV Profiles of Total Extract (TE) vs. 8-Prenylnaringenin (2, 8-PN) and 6-Prenylnaringenin (3, 6-PN)-Knock out Extract (8-PN/6-PN-DE).

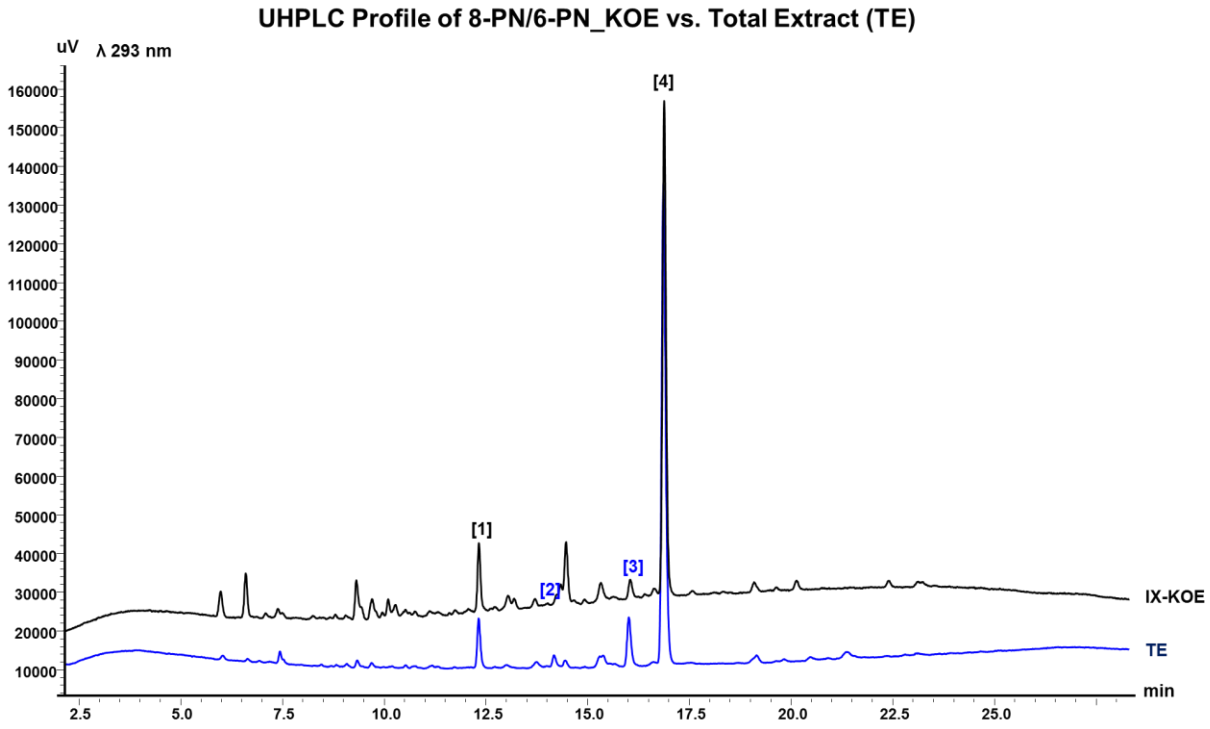

Figure S 10. UHPLC-UV profile of total extract (TE) vs. 8-PN/6-PN-DE. Compounds were eluted on a Waters Acquity UPLC® BEH C18 (2.1 x 5.0 mm, 1.7µm) column using the following gradient A: H_2O, B: MeCN + 0.1% HCO_2H (Formic acid) from 5% to 57% B in 18 min, from 57% to 98 % B in 7 min, isocratic mode at 98 % B and during 3 min at a flow rate of 0.6 mL/ min. Under those conditions, the retention times of (**1**) to (**4**) were 12.2 min, 14.2 min, 16.0 min, and 16.9 min, respectively. In blue, total extract is shown. In black, the respective DE (IX-DE) is shown. Target metabolite **2** and **3** show to be decreased in content from the total extract to produce the DE.

S11. UHPLC UHPLC-UV Profiles of Total Extract (TE) vs. MultiT-DE (Compounds 1-4)

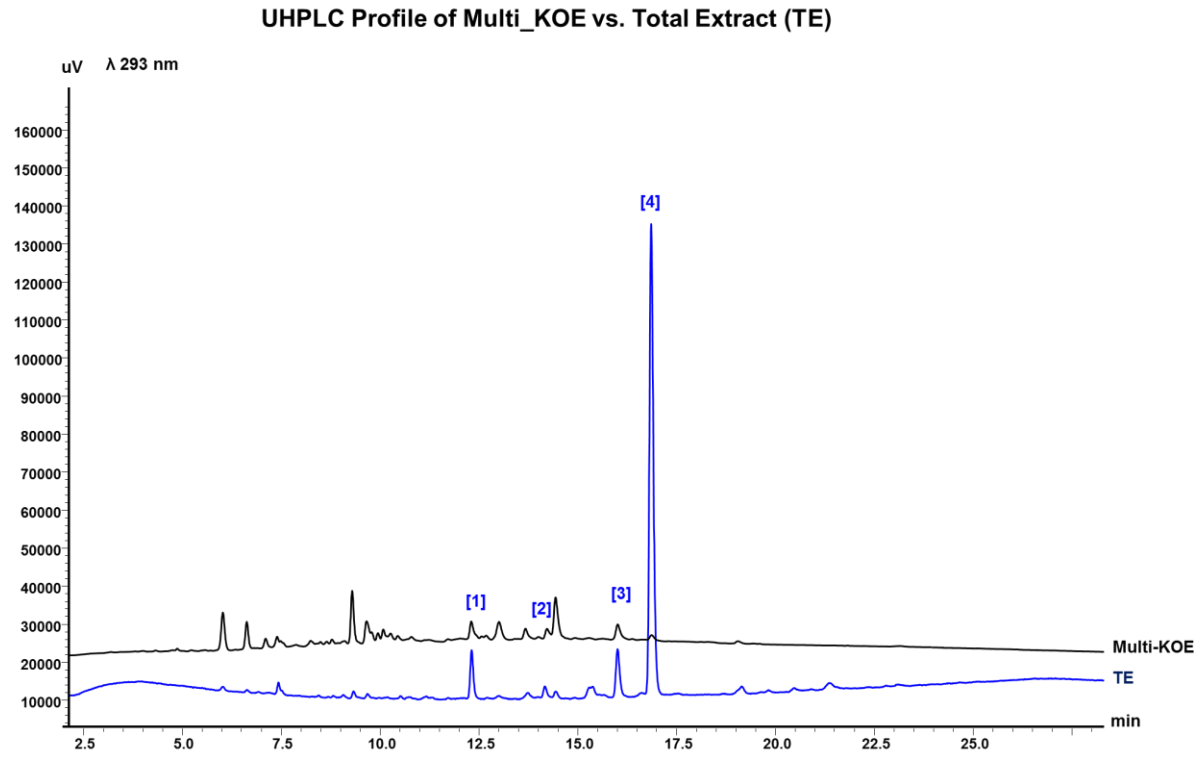

Figure S11. UHPLC-UV profile of total extract (TE) vs. 8-PN/6-PN-DE. Compounds were eluted on a Waters Acquity UPLC® BEH C18 (2.1 x 5.0 mm, 1.7µm) column using the following gradient A: H_2O, B: MeCN + 0.1% HCO_2H (Formic acid) from 5% to 57% B in 18 min, from 57% to 98 % B in 7 min, isocratic mode at 98 % B and during 3 min at a flow rate of 0.6 mL/ min. Under those conditions, the retention times of (**1**) to (**4**) were 12.2 min, 14.2 min, 16.0 min, and 16.9 min, respectively. In blue, the total extract is shown. In black, the respective DE (IX-DE) is shown. Target metabolites **1-4** show to be decreased in content from the total extract to produce the MultiT-DE.

S12. UHPLC-UV Evaluation of the Residual Complexity in the DESIGNER extracts (Ts-DEs)

KOEs	IX % ± SD	%RSD	8-PN % ± SD	%RSD	6-PN % ± SD	%RSD	XH % ± SD	%RSD
XH-KOE	0.58% ± 0.03	0.57	0.01% ± 0.0003	2.95	0.15% ± 0.002	1.22	0.07% ± 0.0005	0.8
IX-KOE	0.07% ± 0.0003	0.41	0.10% ± 0.001	1.15	0.74% ± 0.01	1.39	21.23% ± 0.37	1.78
8-PN/6-PN-KOE	0.83% ± 0.012	1.49	0.20% ± 0.0007	0.38	0.37% ± 0.006	1.67	18.03% ± 0.37	2.06
Multi-KOE	0.08% ± 0.005	7.24	0.04% ± 0.002	6.06	0.10% ± 0.005	5.94	0.10% ± 0.005	5.04

Table S12: UHPLC-UV residual complexity quantification of targeted metabolites in DEs. Compounds were eluted on a Waters Acquity UPLC® BEH C18 (2.1 x 5.0 mm, 1.7µm) column using the following gradient A: H_2O, B: MeCN + 0.1% HCO_2H (Formic acid) from 5% to 57% B in 18 min, from 57% to 98 % B in 7 min, isocratic mode at 98 % B and during 3 min at a flow rate of 0.6 mL/ min. Under those conditions, the retention times of (**1**) to (**4**) were 12.2 min, 14.2 min, 16.0 min, and 16.9 min, respectively. Three measurements were performed per each DE (n=3). The UV wavelengths selected were 293 nm (flavanones) and 369 nm (chalcones). Results are expressed as weight percentages (% w/w) ± the standard deviation (SD). %RSD represents the relative standard deviation in percentage.

S13. Overview of Chemical Engineering of Metabolomic Mixtures

Another approach of targeted design extracts has been done by López, *et al*. with the chemically engineered extracts.[2] Through this alternative approach, natural products extract composition was transformed through chemical diversification[1,2] by targeting chemical functionalities in order to produce semisynthetic natural products-like compound libraries[2,3] with potential and diverse biological activities.[1,3–5] Different functional groups have been targeted, such as carbonyl groups by condensation reaction with hydrazine,[2] and ethanolysis,[5] double bonds and aromatic rings by bromination reaction,[3] and hydroxyl and amine groups by sulfonylation.[4] Subsequent bioassay-guided fractionation of the chemically diversified extracts yielded the antifungal 3(5)-(2,6-dihydroxy-4,5-dimethoxyphenyl)-5(3)-phenylpyrazole,[1] the acetylcholinesterase inhibitor (±)-4',5'-dihydro-5,4',5'-tribromo-8-methyl-psoralen,[3] and the β-glucosidase inhibitors Nα,Nτ-di-benzenesulfonyl histamine,[4] ethyl coumarate,[5] and apigenin.[5]

References

(1) López, S. N.; Ramallo, I. A.; Sierra, M. G.; Zacchino, S. a; Furlan, R. L. E. Chemically Engineered Extracts as an Alternative Source of Bioactive Natural Product-like Compounds. *Proc. Natl. Acad. Sci. U. S. A.* **2007**, *104*, 441–444.

(2) Ramallo, I. A.; Salazar, M. O.; Mendez, L.; Furlan, R. L. E. Chemically Engineered Extracts: Source of Bioactive Compounds. *Acc. Chem. Res.* **2011**, *44*, 241–250.

(3) Méndez, L.; Salazar, M. O.; Ramallo, I. A.; Furlan, R. L. E. Brominated Extracts as Source of Bioactive Compounds. *ACS Comb. Sci.* **2011**, *13*, 200–204.

(4) Salazar, M. O.; Micheloni, O.; Escalante, A. M.; Furlan, R. L. E. Discovery of a B-Glucosidase Inhibitor from a Chemically Engineered Extract Prepared through Sulfonylation. *Mol. Divers.* **2011**, *15*, 713–719.

(5) Ramallo, I. A.; Sierra, M. G.; Furlan, R. L. E. Discovery of B-Glucosidase Inhibitors from a Chemically Engineered Extract Prepared through Ethanolysis. *Med. Chem.* **2012**, *8*, 112–117.

S14. Chemical Subtraction Scheme for *Humulus lupulus* Total Extract

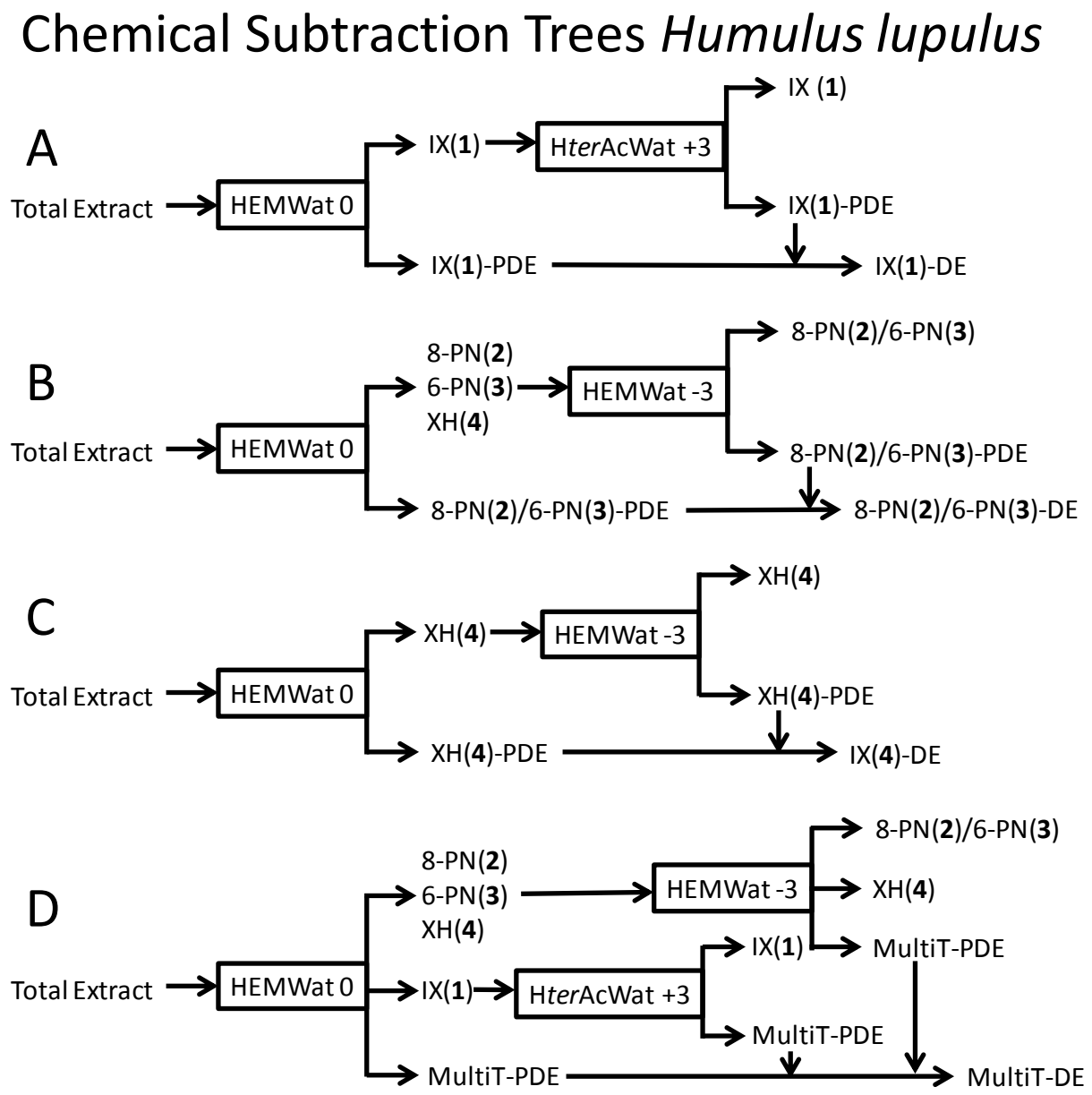

Figure S14: Extraction scheme for the production of six purified subtracted metabolite fractions and four designer extracts (DEs) with nine CS fractionations. Nine Partial DESIGNER Extracts (PDEs) were re-chromatographed and/or combined as indicated.